Kiwi Flavonoids: A Promising Frontier in Breast Cancer Treatment

Aastha Jain
University of Southern California

Abstract

Breast Cancer is a serious health risk that needs to be treated with the right treatments as soon as possible. The study focuses on selecting and analyzing breast cancer target proteins and their interactions with specific ligands, with an emphasis on the anticancer properties of kiwi flavonoids. To identify the breast cancer target proteins, including ABCG2, AKT, CREB1, EGFR, and PI3K, the KEGG Database was utilized. The KEGG Database is a tool for identifying diseases, genes, cellular pathways, and other related entities. Protein structures were retrieved using a resource that can predict protein structures in 3D design, known as AlphaFold. The ligands' binding to the protein structures were retrieved using PubChem, a chemical information library. Ligand preparation involves energy minimization using ChemDraw, which optimizes molecular configurations for enhanced stability. Pharmacophore analysis using Molinspiration and AdmetSAR was employed to identify molecules targeting specific receptors and modulating macromolecular activity, as well as to assess ADME/T properties. Molecular docking was done using CB Dock, a protein-ligand docking website, to predict binding interactions between proteins and ligands. Molecular interaction analysis was conducted using Ligplot, a software program that creates 2D diagrams to visualize intermolecular interactions between proteins and ligands. By performing all of these steps, it was found that kiwi flavonoids, especially the selected ligands, showed anticancer properties. These effects were demonstrated by inhibiting the growth of cancer cells, which ultimately led to cell death. Overall, the findings suggest that kiwi flavonoids can act as therapeutic agents for breast cancer treatment.

Introduction

Breast Cancer is a prevalent type of cancer among women (Cleveland Clinic, 2022). Breast Cancer occurs in the breast tissue. For many years, researchers have been working to gain a deeper understanding of the disease and identify the most effective yet least harmful treatments (Sharma et al., 2010). In this study, various pathways of cancer were researched. One of the pathways studied was the PI3K-AKT pathway, a cellular pathway that advances tumor development and resistance to treatment by regulating other cellular functions involved in cell growth

and survival (PI3K-akt signaling pathway. Cusabio Life Science – Your Biology Science Partner. (n.d.)). Another pathway studied was the RAS/MAPK pathway, which is associated with the epidermal growth factor receptor (EGFR) protein. This pathway promotes cell survival and resistance to drugs by interacting with each other to enhance tumor growth and progression. The next pathway studied is the ATP-binding cassette (ABC) transporter pathway, which is associated with the ABCG2 protein. This pathway expels drugs from chemotherapy treatments out of cancer cells, essentially rendering the treatment ineffective and promoting drug resistance (Ishikawa et al., 2009). Kiwi fruit, also known as Actinidia deliciosa, is originally from New Zealand; however, it is now grown in many other places due to its health benefits, one of which is its anticancer potential (Stonehouse et al., 2013). Kiwis contain flavonoids and antioxidants that contribute to their anticancer potential, as some of these compounds can help prevent cancer growth in the human body. Kiwi antioxidants, such as Vitamin C, can protect DNA from damage that can lead to cancer. Also, since kiwis contain Vitamin C, they help form a healthy immune system to fight off any cancer cells (Collins et al., 2001). In this study, I intend to utilize one of the compounds that contribute to kiwi's anticancer potential, known as flavonoids, and pair it with the breast cancer target proteins chosen for this study to examine their interaction. By doing so, my goal is to determine if kiwi flavonoids can affect the breast cancer target proteins and be a potential candidate for use as a treatment option for breast cancer.

Methodology

Selection of Breast Cancer Target Proteins

The selection of breast cancer target proteins — ABCG2, AKT, EGFR, CREB1, and PI3K — was made with the assistance of the KEGG Database. KEGG is like a library of databases, consisting of diseases, genes, cellular pathways, and more. KEGG is especially well-suited to create pathway maps and molecular networks, making it easier to identify breast cancer target proteins.

Protein Structure Retrieval

When trying to retrieve the structure of each of the five breast cancer target proteins, it is crucial to consult the Protein Data Bank. The protein structures of ABCG2, AKT, EGFR, CREB, and PI3K (Homo sapiens) were predicted using AlphaFold. AlphaFold is a source that can be used to visualize the structure of a protein in a clear 3D design. AlphaFold has essentially predicted the structure of all known proteins on Earth.

Ligand Structure Retrieval

PubChem was used for the retrieval of the following ligand structures: dihydroxyphenylacetic acid, ferulic acid, kaempferol, isoquercetin, and rutin, which bind to ABCG2, AKT, EGFR, CREB, and PI3K. PubChem is like a library for finding chemical information. PubChem also provides the canonical smiles for each ligand, which are then inserted into the Molinspiration search bar to perform pharmacophore analysis.

Ligand Preparation

For ligand preparation, energy minimization was required, and for this purpose, ChemDraw was used. ChemDraw is a tool that allows for the interaction between molecules to be drawn using the canonical smiles provided in PubChem. What happens is, where the molecule present in the environment, it gets a lot of steric hindrances meaning atoms come to too close to each other and causes trouble not being able to find a stable configuration so what chemdraw does is it molds the structure in a way that the configuration that is the most energy minimized is achieved.

Pharmacophore Analysis

Molinspiration and AdmetSAR were used for pharmacophore analysis. Pharmacophore analysis is an efficient and productive method for identifying compounds that can initiate or inhibit the activity of macromolecules. Molinspiration makes use of the ligand's canonical smile. Then, it determines the ligand's characteristics and predicts its bioactivity. AdmetSAR, a database that searches for ADME/T (Absorption, Distribution, Metabolism, Excretion, and Toxicity) qualities based on the canonical values entered for the particular ligand, was also used as part of the pharmacophore study.

Molecular Docking

Molecular docking was performed using CB Dock, a protein-ligand docking website that predicts binding interactions between proteins and ligands. It is easy to use, just go on the website, click dock, download the specific protein(s) and ligand(s), select those files, and click submit where a screen should pop up with the dockings.

Molecular interaction analysis

The molecular interaction analysis was performed using Ligplot. It is a software programming tool that can create a clear representation of the intermolecular interactions between proteins and ligands using 2D diagrams. This way all the information is clearly visible to us. Ligplot shows its qualities, counting hydrogen bonds, and hydrophobic

interactions and other interactions between protein and ligand. The visual diagrams can help with further research in drug design and structure-based drug discovery.

Results

Property	Isoquercetin	Dihydroxyph-enylacetic acid	Ferulic acid	Kaempferol	Rutin
Lipinski rule of 5					
Molecular weight (g/mol)	464.38	168.15	194.19	286.24	610.52
H-bond donor	8	3	2	4	10
H-bond acceptor	12	3	3	6	16
MLogP	-0.54	0.72	1.50	2.28	-1.69
Violations	0	0	0	-	0
Rotatable bonds	4	4	3	-	4
TPSA (Å)	68.15	-	69.25	67.38	65.89
Druglikeness	-	-	-0.58	-	-
Drug score	0.31	-	-	0.47	-
LogS (solubility)	-2.449	-1.149	-2.477	-3.142	-2.772
Synthetic accessibility	-	-	-	-	3.7

TABLE 1. Properties of drugs.

AdmetSAR (Main features. admetSAR. (n.d.)) was used to find the properties of each of the 5 drugs. The properties of drugs can be seen in the table above. The table includes Molecular weight (g/mol) which the values of each drug ranged from 100g/mol to 600g/mol, H-bond donor values ranging from 2-10, H-bond acceptor values ranging from 3-16, MLogP values raining from negative 0 to positive 2.30, Rotatable bonds values going from 1-6, TPSA (A) meaning topological polar surface area values starting from 68.15 of isoquercetin, then nothing for Dihydroxyphenylacetic acid, for Ferulic acid, the TPSA is 69.25, for Kaempferol the value is 67.38 and for Rutin the TPSA is 65.89. The LogS values which is the solubility of each drug range from -1 to -3. The Drug Likeness, Drug Score, and Synthetic accessibility were not easily accessible through AdmetSAR, therefore the values for those components are not available to see in the table above.

AdmetSAR (Main features. admetSAR. (n.d.)) was opted for the pharmacokinetics of Isoquercetin, Dihydroxyphenylacetic acid, Ferulic acid, Kaempferol, and Rutin. In the absorption of these proteins, the components that are available to see are Intestinal absorption, Blood Brain Barrier, which is where the blood-brain exchange happens, oral bioavailability, skin permeation (cm/s), Caco-2 permeability's role is absorption of drugs, P-glycoprotein inhibitor, P-glycoprotein substrate, P-glycoprotein inhibitor and substrate, Plasma protein binding (100%), CYP450 substrate components and CYP450 inhibitor components which are enzymes responsible for metabolizing. In the table below, the CYP450 substrate components are shown as CYP2C9 substrate, CYP3A4 substrate, and CYP2D6 substrate. The CYP450 inhibitor components also can be seen in the table below consisting of CYP3A4 inhibition, CYP2C9 inhibition, CYP2C19 inhibition, CYP2D6 inhibition, CYP1A2 inhibition and CYP inhibitory promiscuity.

Bioactivity	Isoquercetin	Dihydroxyph-enylacetic acid	Ferulic acid	Kaempferol	Rutin
Absorption					
Intestinal absorption	0.5116	0.9073	0.9841	0.9499	0.5564
Blood brain barrier	0.7750	0.5750	0.6500	0.8250	0.8500
Oral bioavailability	0.7286	0.5857	0.6571	0.6286	0.7429
Volume score*	-	-	-	-	-
Skin permeation (cm/s)	0.9122	0.8281	0.7706	0.7817	0.9325
Caco-2 permeability	0.9010	0.6587	0.5801	0.8637	0.9269
P-glycoprotein inhibitior	0.6240	0.9879	0.9866	0.8576	0.6165
P-glycoprotein substrate	0.8086	0.9880	0.9754	0.7327	0.5071
Distribution and Metabolism					
Plasma protein binding (100%)	0.797	0.433	0.727	1.094	0.97

CYP450 substrate					
CYP3A4 substrate	0.6155	0.7847	0.6630	0.5231	0.6398
CYP2C9 substrate	0.6709	0.8012	0.6110	0.6443	0.7038
CYP2D6 substrate	0.8582	0.8218	0.8502	0.8503	0.8611
CYP450 inhibitor					
CYP3A4 inhibition	0.9193	0.9383	0.9240	0.7241	0.9249
CYP2C9 inhibition	0.9296	0.9649	0.5793	0.8948	0.9071
CYP2C19 inhibition	0.9289	0.9743	0.6276	0.6434	0.9025
CYP2D6 inhibition	0.9513	0.9257	0.9588	0.9083	0.9545
CYP1A2 inhibition	0.9084	0.9513	0.7513	0.9108	0.8673
CYP inhibitory promiscuity	0.7728	0.9593	0.7745	0.7652	0.6787

TABLE 2. Pharmacokinetics.

Bioactivity	Isoquercetin	Dihydroxyp-henylacetic acid	Ferulic acid	Kaempferol	Rutin
Kinase inhibitor	-0.59	-0.29	-0.45	-0.67	-0.59
Nuclear receptor ligand	0.6533	0.7077	0.7400	0.9400	0.7192
Enzyme inhibitor	0.9265	0.9608	0.8757	0.7689	0.8956
Estrogen receptor binding	0.7470	0.7853	0.5509	0.8946	0.7901
Androgen receptor binding	0.7633	0.5275	0.5836	0.9001	0.6176
Thyroid receptor binding	0.5202	0.7692	0.7859	0.6393	0.5312

Glucocorticoid receptor binding	0.7040	0.6374	0.6863	0.9172	0.6215
Aromatase binding	0.5913	0.7807	0.8404	0.9089	0.6273

TABLE 3. Absorption, distribution, and metabolism of drugs.

Again, Admetsar (Main features. admetSAR. (n.d.)) was used for the toxicity analysis of Isoquercetin, Dihydroxyphenylacetic acid, Ferulic acid, Kaempferol, and Rutin. The components that they got data for is acute oral toxicity which the values for each drug were between the 0-1 range, Hepatotoxicity which the values happened to be all in the 0 range, Mutagenesis which happened to be between the 0.50 to 1 range, Carcinogenicity which also happened to be between 0 to 1, irritants ranging from 0.70 to 0.90, eye irritation values ranging from 0.70 to 1, eye corrosion values ranging from 0.40 to 1, reproductive effect, Human ether-a-go-go (hERT) inhibition values going from 0.30 to 1, Tetrahymena pyriformis toxicity values ranging from 0.40 to 0.70, and Genotoxicity values ranging from 0.50 to 0.80.

Toxicity	Isoquercetin	Dihydroxyphenyl acetic acid	Ferulic acid	Kaempferol	Rutin
Acute oral toxicity	0.4045	1.6743	1.4395	1.8298	0.5971
Hepatotoxicity	0.5196	0.5375	0.8500	0.6125	0.6625
Mutagenesis	0.7200	0.7600	0.9600	0.7700	0.5500
Carcinogenicity	1.0000	0.7900	0.7197	1.0000	1.0000
Irritant	0.7144	0.8455	0.7685	0.8634	0.8687
Eye irritation	0.7321	1.0000	0.9932	0.9669	0.8973
Eye corrosion	0.9930	0.8875	0.4644	0.9903	0.9922
Reproductive effect	0.7568	0.6333	0.7889	0.7667	0.7667
Human either-a-go-go (hERT) inhibition	0.5000	0.8557	0.7574	0.9143	0.3823
Tetrahymena pyriformis toxicity	0.659	-0.579	0.48	1.77	0.716
Genotoxicity	0.7865	0.6842	0.7358	0.5678	0.6768

TABLE 4. Toxicity analysis of drugs.

Molecular docking

CB Dock (CB-dock. An accurate protein-ligand blind docking tool. (n.d.)) was used to get these images. A. Chemical structure of Isoquercetin containing four hydroxide and four oxygen molecules. B. Chemical structure of Dihydroxyphenylacetic acid containing 2 hydroxide molecules and 1 oxygen molecule. Chemical structure of ferulic acid containing 1 hydroxide molecule and 2 oxygen molecules. The chemical structure of Kaempferol has 2 hydroxide and 2 oxygen molecules. The chemical structure of rutin has 4 hydroxide molecules and 6 oxygen molecules.

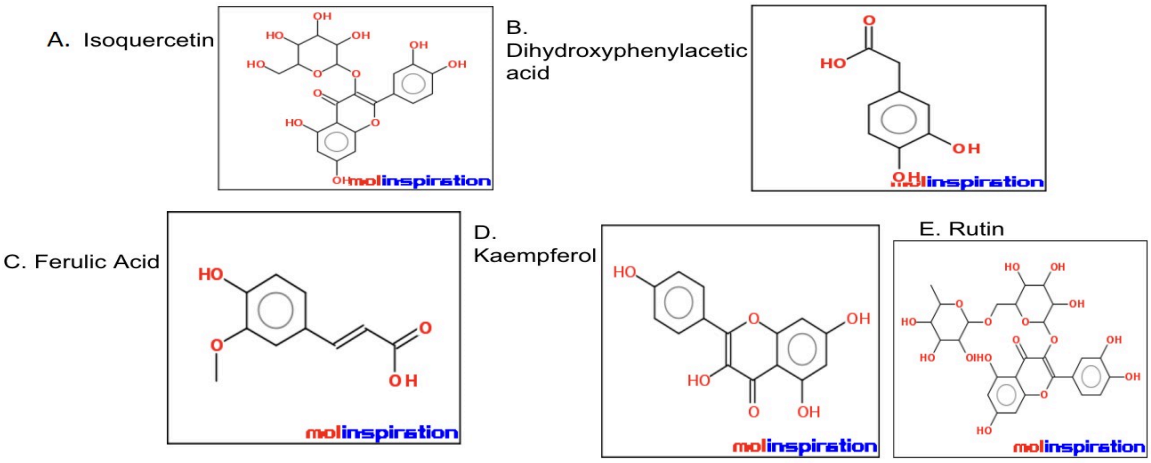

FIGURE 1. Chemical structure of the drugs.

CB Dock (CB-dock. An accurate protein-ligand blind docking tool. (n.d.)) was used to get these images. Figure 2 a. shows images of protein - ligand interaction between Abcg2 and Dihydroxyphenylacetic acid. Figure 2 b. shows protein-ligand interaction between Abcg2 and Ferulic acid. Figure 2 c. shows protein-ligand interaction between Abcg2 and Isoquercetin. Figure 2 d. shows protein-ligand interaction between Abcg2 and Kaempferol. Lastly Figure 2 e. shows protein-ligand interaction between Abcg2 and Rutin.

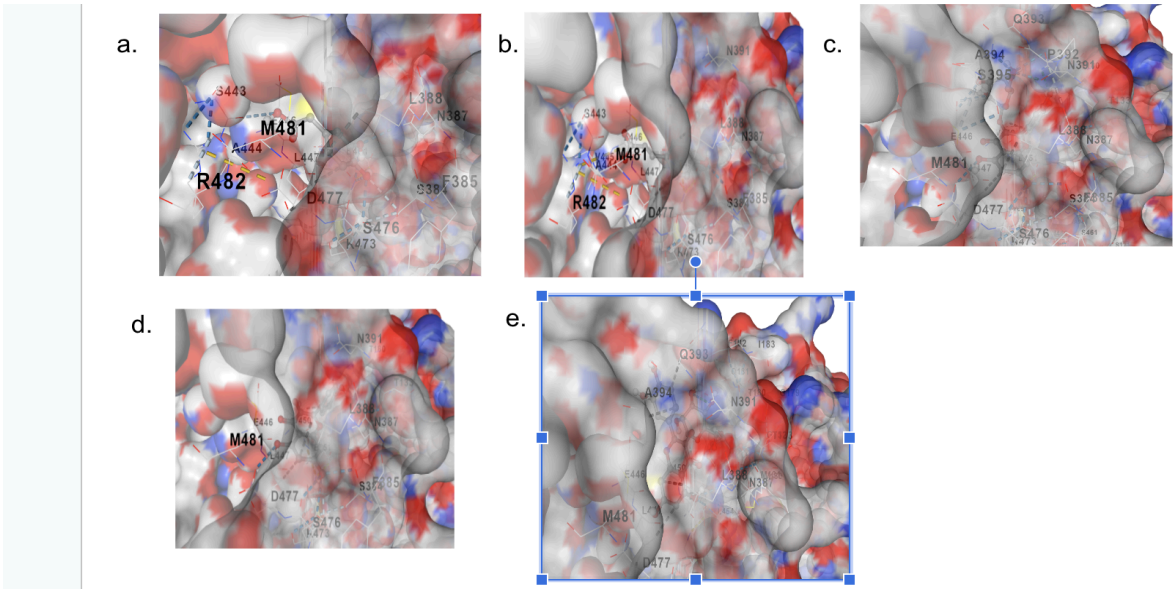

FIGURE 2. ABCG2 and ligand interaction.

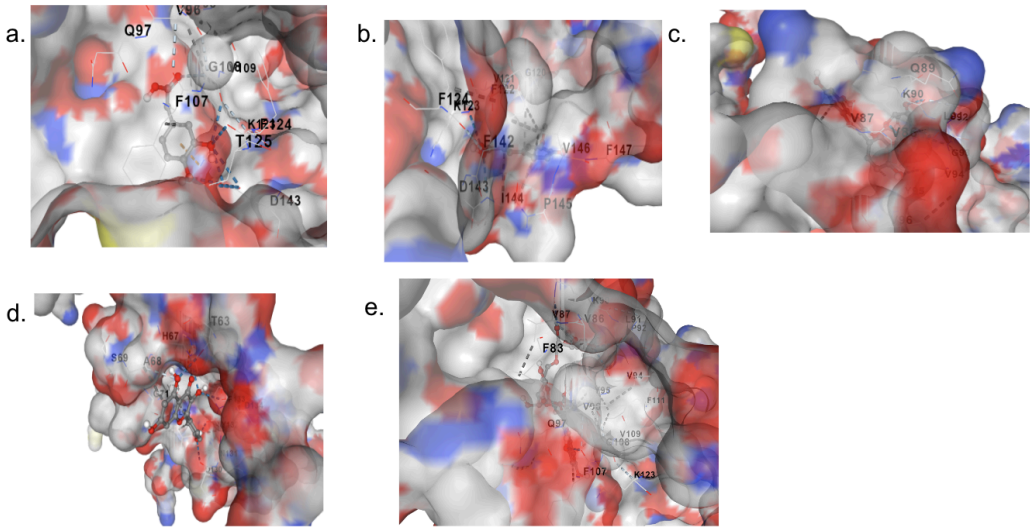

FIGURE 3. AKT and ligand interaction.

CB Dock (CB-dock. An accurate protein-ligand blind docking tool. (n.d.)) was used to get these images. Figure 3 a. shows images of the protein - ligand interaction between AKT and Dihydroxyphenylacetic acid. Figure 3 b. shows protein-ligand interaction between AKT and Ferulic acid. Figure 3 c. shows protein-ligand interaction between AKT and Isoquercetin. Figure 3 d. shows protein-ligand interaction between AKT and kaempferol. Lastly Figure 3 e. shows the protein-ligand interaction between AKT and Rutin.

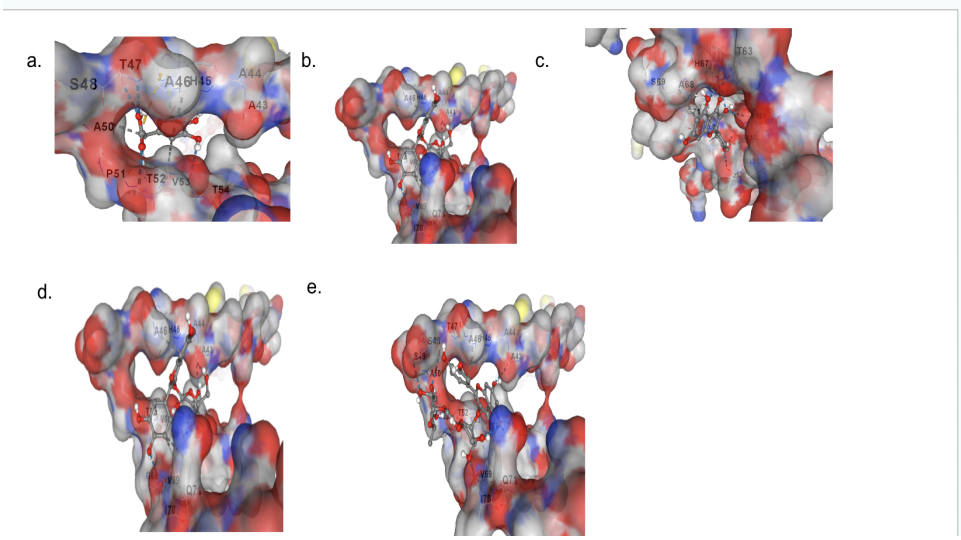

FIGURE 4. CREB and ligand interaction.

CB Dock (CB-dock. An accurate protein-ligand blind docking tool. (n.d.)) was used to get these images. Figure 4 a. shows images of the protein - ligand interaction between CREB and Dihydroxyphenylacetic acid. Figure 4 b. shows protein-ligand interaction between CREB and Ferulic acid. Figure 4 c. shows protein-ligand interaction between CREB and Isoquercetin. Figure 4 d. shows protein-ligand interaction between CREB and Kaempferol. Lastly Figure 4 e. shows protein-ligand interaction between CREB and Rutin.

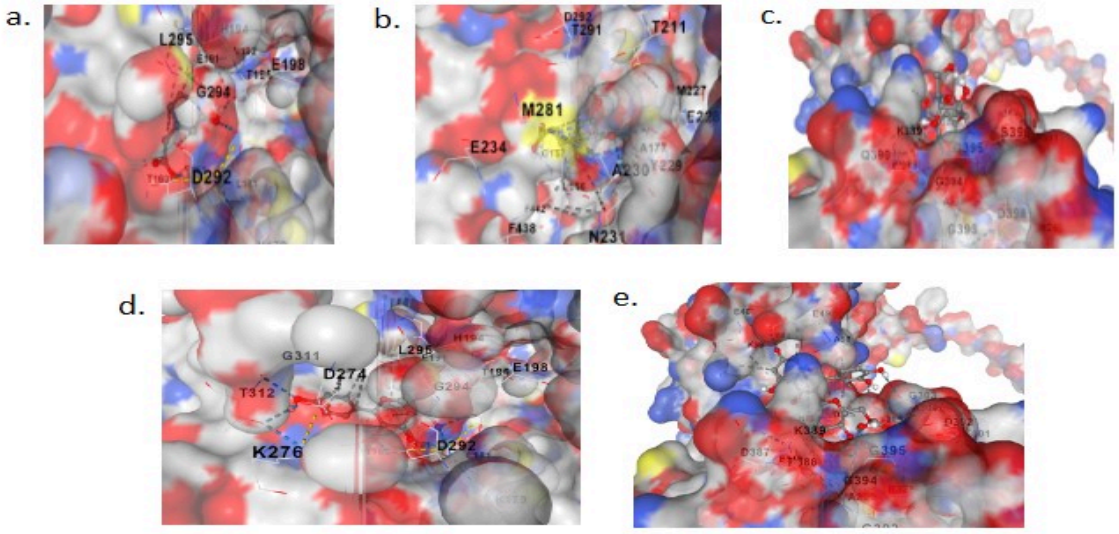

FIGURE 5. EGFR and ligand interaction.

CB Dock (CB-dock. An accurate protein-ligand blind docking tool. (n.d.)) was used to get these images. Figure 5 a. shows images of the protein - ligand interaction between EGFR and Dihydroxyphenylacetic acid. Figure 5 b. shows protein-ligand interaction between EGFR and Ferulic acid. Figure 5 c. shows protein-ligand interaction between EGFR and Isoquercetin. Figure 5 d. shows protein-ligand interaction between EGFR and Kaempferol. Lastly Figure 5 e. shows protein-ligand interaction between EGFR and Rutin.

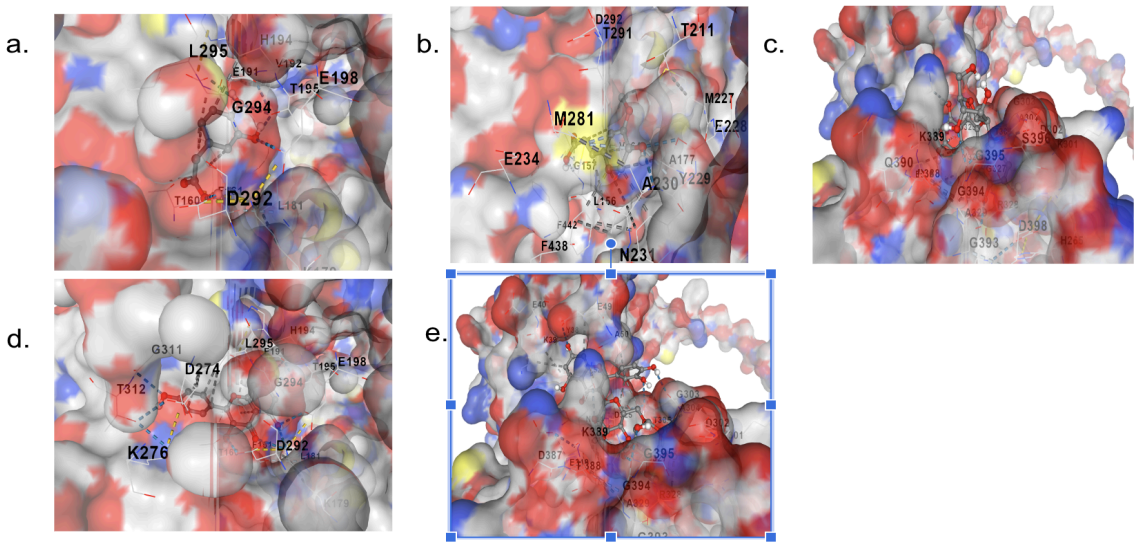

FIGURE 6. PI3K and ligand interaction.

CB Dock (CB-dock. An accurate protein-ligand blind docking tool. (n.d.)) was used to get these images. Figure 6 a. shows images of the protein - ligand interaction between PI3K and Dihydroxyphenylacetic acid. Figure 6 b. shows protein-ligand interaction between PI3K and Ferulic acid. Figure 6 c. shows protein-ligand interaction between PI3K and Isoquercetin. Figure 6 d. shows protein-ligand interaction between PI3K and Kaempferol. Lastly Figure 6 e. shows protein-ligand interaction between PI3K and Rutin.

To see the protein-ligand interaction in 2-D images, Ligplot (Team, E. W., n.d.). Ligplot+ v.2.2 - ligand-protein interaction diagrams) was used, which is a software where close-up interactions are visible. As shown in Table 1, Dihydroxyphenylacetic acid and Pi3k have 19 hydrophobic interactions and 2 hydrogen bonds. There are 25 hydrophobic interactions between ferulic acid and Pi3k, as well as 2 hydrogen bonds. Isoquercetin and Pi3k gave 16 hydrophobic interactions and 6 hydrogen bonds. Kaempferol and Pi3k have 32 hydrophobic interactions and 3 hydrogen bonds. Rutin and Pi3k have 20 hydrophobic interactions and 7 hydrogen bonds.

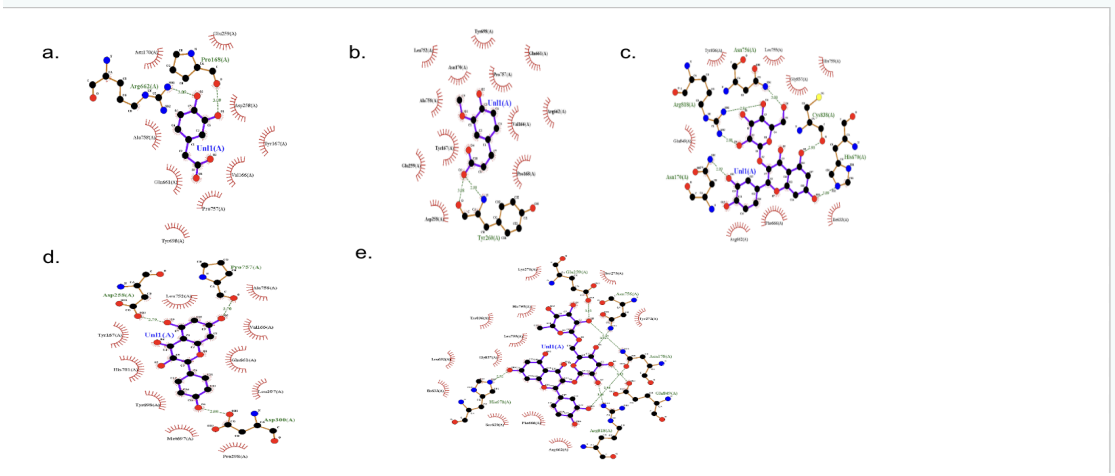

Interaction	No. of Hydrophobic Interactions	No. of Hydrogen Bonds
Dihydroxyphenylacetic_acid_pi3k	19	2
Ferulic_acid_Pi3k	25	2
Isoquercetin_Pi3k	16	6
Kaempferol_Pi3k	32	3
Rutin_2d_Pi3k	20	7

TABLE 1. PI3K.

Ligplot (Team, E. W. (n.d.). Ligplot+ v.2.2 - ligand-protein interaction diagrams) was again used to show the hydrophobic interactions and hydrogen bonds between protein and ligand. As shown in Table 2, Dihydroxyphenylacetic acid and abcg2 have 11 hydrophobic interactions and 5 hydrogen bonds. There are 18 hydrophobic interactions between ferulic acid and ABCG2, as well as 4 hydrogen bonds. Isoquercetin and abcg2 gave 13 hydrophobic interactions and 8 hydrogen bonds. Kaempferol and abcg2 have 16 hydrophobic interactions and 4 hydrogen bonds. Rutin and abcg2 have 14 hydrophobic interactions and 8 hydrogen bonds.

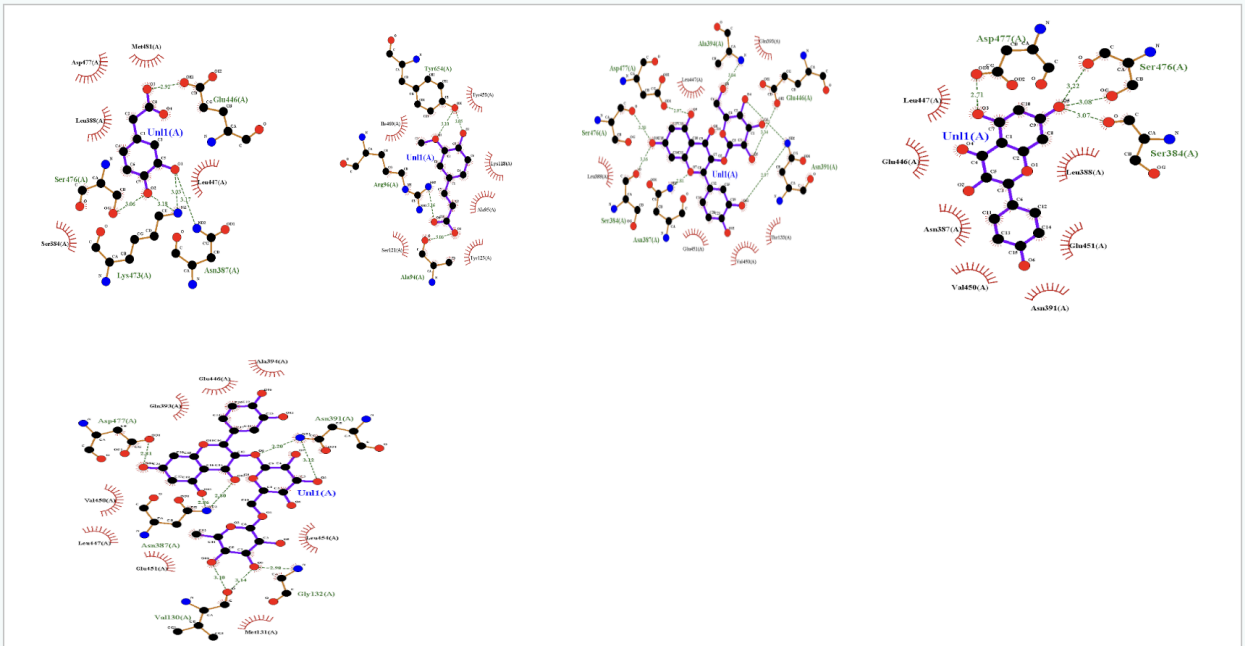

Interaction	No. of Hydrophobic Interactions	No. of Hydrogen Bonds
Dihydroxyphenylacetic_acid_ABCG2	11	5
Ferulic_acid_ ABCG2	18	4
Isoquercetin_ ABCG2	13	8
Kaempferol_ ABCG2	16	4
Rutin_2d_ ABCG2	14	8

TABLE 2. ABCG2.

Ligplot (Team, E. W., n.d.). Ligplot+ v.2.2 - ligand-protein interaction diagrams was also used here. As shown in Table 3, AKT has 12 hydrophobic interactions and 3 hydrogen bonds. There are 21 hydrophobic interactions between ferulic acid and AKT, as well as 2 hydrogen bonds. Isoquercetin and AKT gave 11 hydrophobic interactions and 6 hydrogen bonds. Kaempferol and AKT have 10 hydrophobic interactions and 5 hydrogen bonds. Rutin and AKT have 17 hydrophobic interactions and 7 hydrogen bonds.

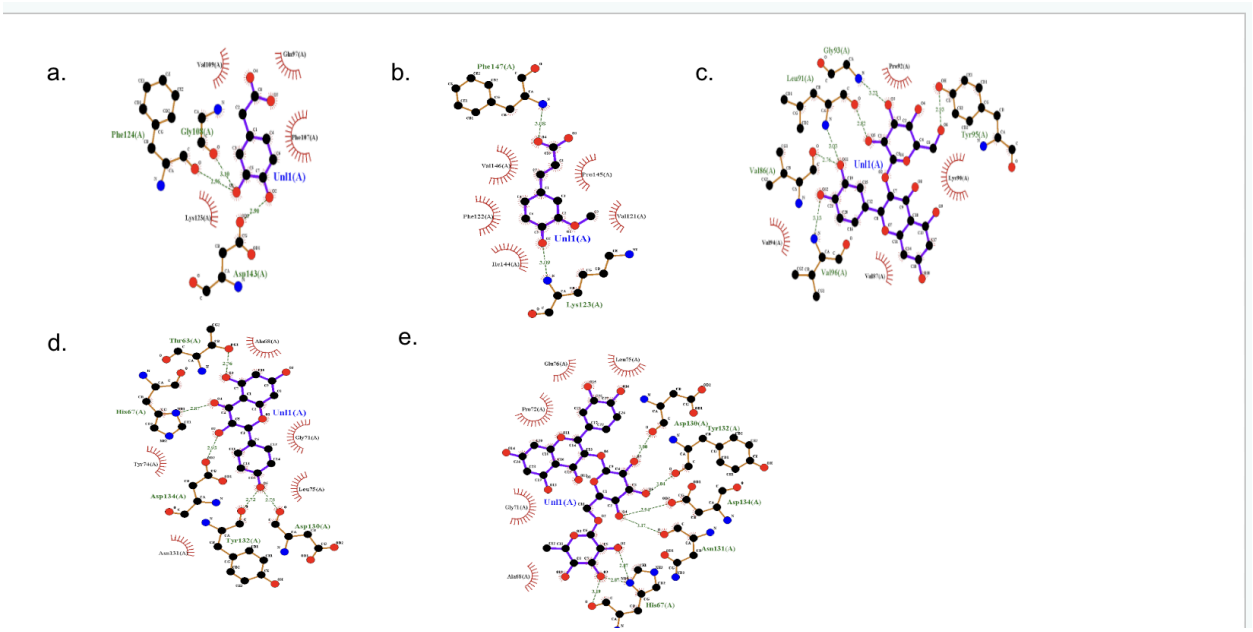

Interaction	No. of Hydrophobic Interactions	No. of Hydrogen Bonds
Dihydroxyphenylacetic_acid_AKT	12	3
Ferulic_acid_ AKT	21	2
Isoquercetin_ AKT	11	6
Kaempferol_ AKT	10	5
Rutin_2d_ AKT	17	7

TABLE 3. AKT.

Ligplot (Team, E. W., n.d.). Ligplot+ v.2.2 - ligand-protein interaction diagrams were used here. As shown in Table 4, Dihydroxyphenylacetic acid and creb1 have 10 hydrophobic interactions and four hydrogen bonds. There are four hydrophobic interactions between ferulic acid and CREB1, and five hydrogen bonds. Isoquercetin and creb1 gave 15 hydrophobic interactions and 5 hydrogen bonds. Kaempferol and creb1 have 14 hydrophobic interactions and 4 hydrogen bonds. Rutin and creb1 have 11 hydrophobic interactions and 9 hydrogen bonds.

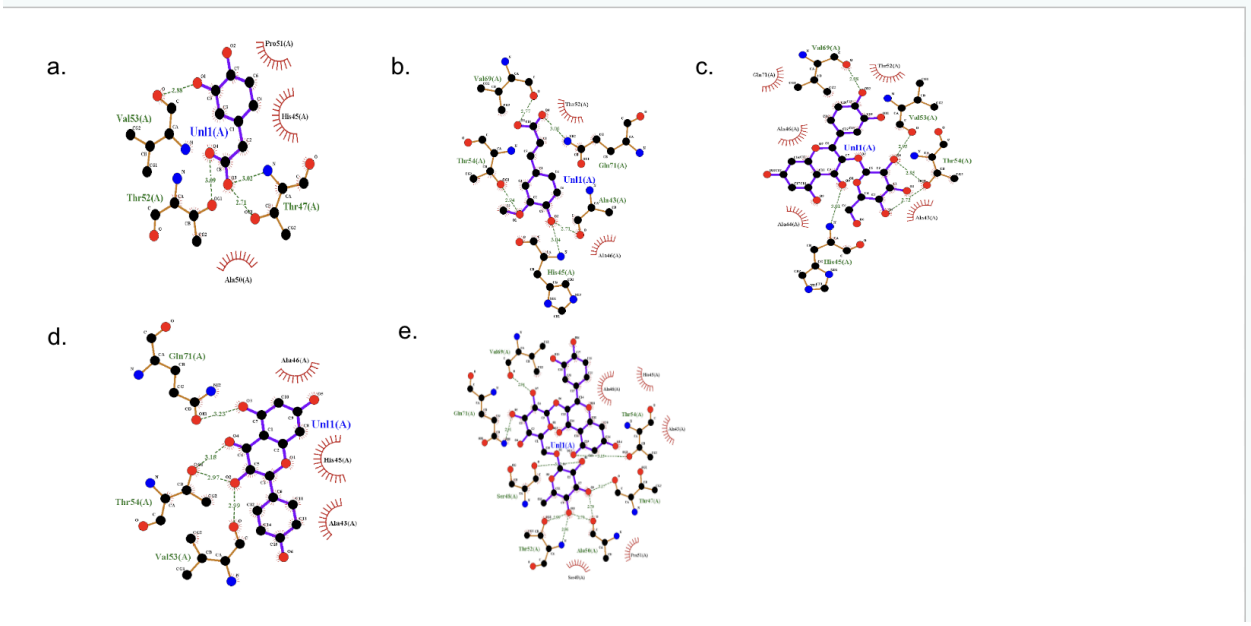

Interaction	No. of Hydrophobic Interactions	No. of Hydrogen Bonds
Dihydroxyphenylacetic_acid_CREB1	10	4
Ferulic_acid_ CREB1	4	5
Isoquercetin_ CREB1	15	5
Kaempferol_ CREB1	14	4
Rutin_2d_ CREB1	11	9

TABLE 4. CREB.

Ligplot (Team, E. W., n.d.). Ligplot+ v.2.2 - ligand-protein interaction diagrams was used here. As shown in Figure 11, Dihydroxyphenylacetic acid and EGFR have 16 hydrophobic interactions and 4 hydrogen bonds. There are 22 hydrophobic interactions between ferulic acid and EGFR, as well as 2 hydrogen bonds. Isoquercetin and EGFR gave 31 hydrophobic interactions and 2 hydrogen bonds. Kaempferol and EGFR have 16 hydrophobic interactions and 6 hydrogen bonds. Rutin and EGFR have 27 hydrophobic interactions and 7 hydrogen bonds.

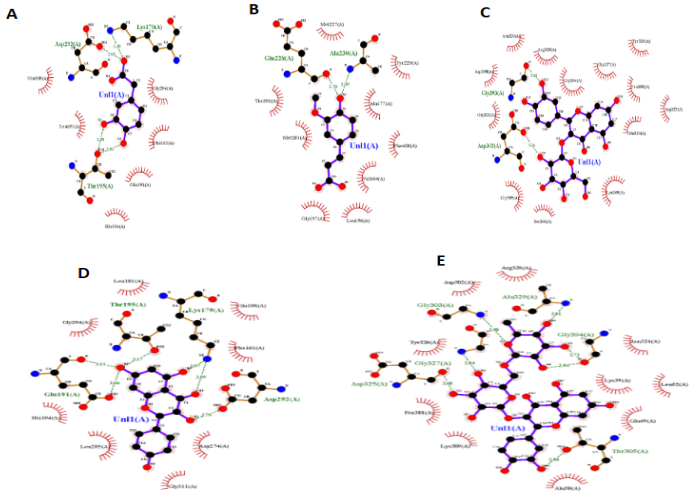

Interaction	No. of Hydrophobic Interactions	No. of Hydrogen Bonds
Dihydroxyphenylacetic_acid_EGFR	16	4
Ferulic_acid_ EGFR	22	2
Isoquercetin_ EGFR	31	2
Kaempferol_ EGFR	16	6
Rutin_2d_ EGFR	27	7

TABLE 5. EGFR.

Discussion

Breast cancer is a worry for women all around the world. Scientists and researchers like me are working hard to find ways to make life better for breast cancer patients, and one of their main goals is to find a proper treatment for breast cancer with minimal side effects and better affordability/accessibility. Just as Ixabepilone (Ixempra) drug in our research is used to treat breast cancer and the goal here is to try to advance that to treat metastatic breast cancer, others are facing the problem of what form of treatment to use in case other individuals dealing with breast cancer get tired from all the treatment options they have tried. In such

cases, others are trying to develop a new type of treatment that is effective for those patients.

Radiation therapy is also one of the treatment options that many breast cancer patients have tried. There are also different types of cancer. Just as breast cancer is researched here, another type of cancer to relate this to is called melanoma, which affects the skin, and kiwi fruit has been shown to provide antitumor effects to the affected cells. It has been observed to act as a radiosensitizer in melanoma cells, making it a viable form of treatment. Isoquercetin, Dihydroxyphenylacetic acid, Ferulic Acid, Rutin, and Kaempferol are the selected flavonoids of kiwi, which are compounds that provide anticancer properties in plants; therefore, these were chosen for study. Isoquercetin prevents cell proliferation in melanoma cells, which are associated with skin cancer. Kaempferol acts as a chemotherapeutic agent against skin cancer. Ferulic acid prevents cell proliferation in cervical cancer cells. Rutin causes cell death, also known as apoptosis, in colon cancer cells.

Pharmacokinetic analysis is crucial in drug discovery, as it enables the optimization of ADME (absorption, distribution, metabolism, and excretion) features to achieve the desired efficacy and safety profiles. In pharmacokinetic analysis, drug molecules interact with the body to control various processes. It is important in drug discovery because it shows how the body interacts with the drug.

AdmetSAR was picked for the pharmacokinetics of Isoquercetin, Dihydroxyphenylacetic acid, Ferulic acid, Kaempferol, and Rutin. Within the absorption of these proteins, the components that are accessible to see are Intestinal absorption, Blood Brain Barrier which is where the blood-brain trade happens, oral bioavailability, skin penetration (cm/s), Caco-2 permeability's role is absorption of drugs, P-glycoprotein inhibitor, P-glycoprotein substrate, P-glycoprotein inhibitor and substrate, Plasma protein binding (100%), CYP450 substrate components and CYP450 inhibitor components which are enzymes responsible for metabolizing. Within Table 2, the CYP450 substrate components are listed as CYP3A4 substrate, CYP2C9 substrate, and CYP2D6 substrate. The CYP450 inhibitor components are also listed in Table 2, which includes CYP3A4 inhibition, CYP2C9 inhibition, CYP2C19 inhibition, CYP2D6 inhibition, CYP1A2 inhibition, and CYP inhibitory promiscuity.

AdmetSAR was selected for the toxicity analysis of Isoquercetin, Dihydroxyphenylacetic acid, Ferulic acid, Kaempferol, and Rutin. The components for which AdmetSAR obtained data include acute oral toxicity, hepatotoxicity, mutation, carcinogenicity, irritants, eye irritation, eye corrosion, reproductive effects, Human ether-a-go-go (hERG) inhibition, Tetrahymena pyriformis toxicity, and genotoxicity. ABCG2 has been identified in various tissues, including the placenta. ABCG2 is involved in metabolizing lipids in macrophages. It acts as a multidrug-resistance protein from a breast cancer cell line. Overall, the ABCG2 protein acts as a transporter to eliminate toxins from the body,

and it is also known as a breast cancer resistance protein. The PI3K and Akt proteins play a crucial role in regulating cell survival and death. The EGFR protein is also known as the Epidermal Growth Factor Receptor. The role of the EGFR protein is similar to that of technology, in that both facilitate communication between two stimuli. The phone enables communication between two individuals, and the EGFR protein facilitates cell communication. CREB1 protein is a marker for breast cancer. CREB1 protein helps determine if a person has breast cancer by assessing whether the patient's CREB1 levels have increased. CREB1 levels are typically increased in patients with metastatic disease. This protein shows the spread of the disease within the body.

Molecular docking is a good way to understand how protein-ligand interactions work. Ligplot is a software tool that creates a clear representation of the intermolecular interactions between proteins and ligands, including their qualities, such as hydrogen bonds and hydrophobic interactions. In the PI3K protein, we saw that diacid and PI3K have 19 hydrophobic interactions and 2 hydrogen bonds. There are 25 hydrophobic interactions between ferulic acid and Pi3k, as well as 2 hydrogen bonds. Isoquercetin and Pi3k gave 16 hydrophobic interactions and 6 hydrogen bonds. Kaempferol and Pi3k have 32 hydrophobic interactions and 3 hydrogen bonds. Rutin and Pi3k have 20 hydrophobic interactions and 7 hydrogen bonds. In the ABCG2 protein, we observed that Dihydroxyphenylacetic acid and ABCG2 exhibit 11 hydrophobic interactions and 5 hydrogen bonds. There are 18 hydrophobic interactions between ferulic acid and ABCG2, as well as 4 hydrogen bonds. Isoquercetin and abcg2 gave 13 hydrophobic interactions and 8 hydrogen bonds. Kaempferol and abcg2 have 16 hydrophobic interactions and 4 hydrogen bonds. Rutin and Abcg2 have 14 hydrophobic interactions and 8 hydrogen bonds. In AKT protein, there are 21 hydrophobic interactions within ferulic acid and Akt and 2 hydrogen bonds. Isoquercetin and Akt gave 11 hydrophobic interactions and 6 hydrogen bonds. Kaempferol and Akt have 10 hydrophobic interactions and 5 hydrogen bonds. Rutin and Akt have 17 hydrophobic interactions and 7 hydrogen bonds. In the CREB protein, we observed 10 hydrophobic interactions and 4 hydrogen bonds between dihydroxyphenylacetic acid and CREB1. There are four hydrophobic interactions between ferulic acid and CREB1, and five hydrogen bonds. Isoquercetin and creb1 gave 15 hydrophobic interactions and 5 hydrogen bonds. Kaempferol and creb1 have 14 hydrophobic interactions and 4 hydrogen bonds. Rutin and creb1 have 11 hydrophobic interactions and 9 hydrogen bonds. Lastly, in the EGFR protein, we observed 16 hydrophobic interactions and 4 hydrogen bonds between Dihydroxyphenylacetic acid and EGFR. There are 22 hydrophobic interactions between ferulic acid and EGFR, as well as 2 hydrogen bonds. Isoquercetin and EGFR gave 31 hydrophobic interactions and 2 hydrogen bonds. Kaempferol and EGFR have 16 hydrophobic interactions and 6

hydrogen bonds. Rutin and EGFR have 27 hydrophobic interactions and 7 hydrogen bonds.

Conclusion

ABCG2 is a multidrug resistance protein. It is associated with the various hallmarks of cancer and it is composed of natural compounds. There is a drug called Ixabepilone (Ixempra) to treat locally advanced or metastatic breast cancer. However, there are side effects to this drug, like any other drug, and so to counteract the side effects of this drug, we have come up with a cost-efficient solution, which has minimal side effects. I have found that the kiwi fruit found in local grocery stores contains flavonoids that provide anti-cancer properties, with the ability to inhibit cancer cell growth and induce cell death. Therefore, kiwi flavonoids can work as therapeutic agents for breast cancer treatment.

References

Experimental immunotherapy targets metastatic breast cancer. National Cancer Institute. (n.d.). Retrieved April 9, 2023, from https://www.cancer.gov/news-events/press-releases/2022/personalized-immunotherapy-metastatic-breast-cancer

February 23, 2023, January 20, 2023, & March 9, 2023. (n.d.). Shorter radiation course for some with early breast cancer. National Cancer Institute. Retrieved April 9, 2023, from https://www.cancer.gov/news-events/cancer-currents-blog/2022/early-breast-cancer-shorter-radiation-therapy

Lippi, G., & Mattiuzzi, C. (2020). Kiwifruit and Cancer: An Overview of Biological Evidence. Nutrition and cancer, 72(4), 547–553. https://doi.org/10.1080/01635581.2019.1650190

Kou, L., Zhu, Z., Fajardo, E., Bai, Q., Redington, C., Xiao, H., Lequio, M., Sham, N., Wakefield, M. R., & Fang, Y. (2021). Harnessing the Power of Kiwifruit for Radiosensitization of Melanoma. Anticancer research, 41(12), 5945–5951. https://doi.org/10.21873/anticanres.15413

Won, Y. S., Kim, J. H., Lizardo, R. C. M., Min, H. J., Cho, H. D., Hong, S. M., & Seo, K. I. (2020). The Flavonol Isoquercitrin Promotes Mitochondrial-Dependent Apoptosis in SK-Mel-2 Melanoma Cells via the PI3K/AKT/mTOR Pathway. Nutrients, 12(12), 3683. https://doi.org/10.3390/nu12123683

Lee, K. M., Lee, K. W., Jung, S. K., Lee, E. J., Heo, Y. S., Bode, A. M., Lubet, R. A., Lee, H. J., & Dong, Z. (2010). Kaempferol inhibits UVB-induced COX-2 expression by suppressing Src kinase activity. Biochemical pharmacology, 80(12), 2042–2049. https://doi.org/10.1016/j.bcp.2010.06.042

Gao, J., Yu, H., Guo, W., Kong, Y., Gu, L., Li, Q., Yang, S., Zhang, Y., & Wang, Y. (2018). The anticancer effects of ferulic acid is associated with induction of cell cycle arrest and autophagy in cervical cancer cells. Cancer Cell International, 18, 102. https://doi.org/10.1186/s12935-018-0595-y

Pandey, P., Khan, F., Qari, H. A., & Oves, M. (2021). Rutin (Bioflavonoid) as Cell Signaling Pathway Modulator: Prospects in Treatment and Chemoprevention. Pharmaceuticals (Basel, Switzerland), 14(11), 1069. https://doi.org/10.3390/ph14111069

Reichel, A., & Lienau, P. (2016). Pharmacokinetics in Drug Discovery: An Exposure-Centred Approach to Optimising and Predicting Drug Efficacy and Safety. Handbook of experimental pharmacology, 232, 235–260. https://doi.org/10.1007/164_2015_26

Glassman, P. M., & Muzykantov, V. R. (2019). Pharmacokinetic and Pharmacodynamic Properties of Drug Delivery Systems. The Journal of pharmacology and experimental therapeutics, 370(3), 570–580. https://doi.org/10.1124/jpet.119.257113

Hinz, N., & Jücker, M. (2019). Distinct functions of AKT isoforms in breast cancer: a comprehensive review. Cell communication and signaling: CCS, 17(1), 154. https://doi.org/10.1186/s12964-019-0450-3

Yurong Lai, & Abstract: BCRP contains only six transmembrane helices and one nucleotide-binding domain located toward the N terminus. (2014, September 12). Breast cancer resistance protein (BCRP)/ABCG2. Transporters in Drug Discovery and Development. Retrieved April 9, 2023, https://www.sciencedirect.com/science/article/pii/B9781907568213500 4X

Basu, A., & Lambring, C. B. (2021). Akt Isoforms: A Family Affair in Breast Cancer. Cancers, 13(14), 3445. https://doi.org/10.3390/cancers13143445

Paplomata, E., & O'Regan, R. (2014). The PI3K/AKT/mTOR pathway in breast cancer: targets, trials and biomarkers. Therapeutic advances in medical oncology, 6(4) 154–166. https://doi.org/10.1177/1758834014530023

Steven, A., & Seliger, B. (2016). Control of CREB expression in tumors: from molecular mechanisms and signal transduction pathways to therapeutic targets. Oncotarget, 7(23), 35454–35465. https://doi.org/10.18632/oncotarget.7721

Sigismund, S., Avanzato, D., & Lanzetti, L. (2018). Emerging functions of the EGFR in cancer. Molecular oncology, 12(1), 3–20. https://doi.org/10.1002/1878-0261.12155

Morris, G. M., & Lim-Wilby, M. (2008). Molecular docking. Methods in molecular biology (Clifton, N.J.), 443, 365–382. https://doi.org/10.1007/978-1-59745-177-2_19

Durhan, B., Yalçın, E., Çavuşoğlu, K. et al. Molecular docking assisted biological functions and phytochemical screening of Amaranthus lividus L. extract. Sci Rep 12, 4308 (2022). https://doi.org/10.1038/s41598-022-08421-8

Woodward, O. M., Köttgen, A., & Köttgen, M. (2011). ABCG transporters and disease. The FEBS journal, 278(18), 3215–3225. https://doi.org/10.1111/j.1742-4658.2011.08171.x

Calculation of molecular properties and bioactivity score. (n.d.). https://www.molinspiration.com/cgi-bin/properties

CB-dock. CB-Dock: An accurate protein-ligand blind docking tool. (n.d.). http://clab.labshare.cn/cb-dock/php/blinddock.php

Database, A. P. S. (n.d.). Alphafold protein structure database. AlphaFold Protein Structure Database. https://alphafold.ebi.ac.uk/

KEGG pathway database. (n.d.). https://www.genome.jp/kegg/pathway.html

Main features. admetSAR. (n.d.). http://lmmd.ecust.edu.cn/admetsar2

U.S. National Library of Medicine. (n.d.). PubChem. National Center for Biotechnology Information. PubChem Compound Database. https://pubchem.ncbi.nlm.nih.gov/

Team, E. W. (n.d.). Ligplot+ v.2.2 - ligand-protein interaction diagrams. LigPlot+ home page. https://www.ebi.ac.uk/thornton-srv/software/LigPlus/

Cleveland Clinic. (2022, January 21). Breast Cancer: Causes, Stage, Diagnosis & Treatment. Cleveland Clinic. https://my.clevelandclinic.org/health/diseases/3986-breast-cancer

Sharma, G. N., Dave, R., Sanadya, J., Sharma, P., & Sharma, K. K. (2010). Various Types and Management of Breast Cancer: An Overview. Journal of advanced pharmaceutical technology & research, 1(2), 109–126

PI3K-akt signaling pathway. Cusabio Life Science – Your Biology Science Partner. (n.d.). https://www.cusabio.com/pathway/PI3K-Akt-signaling-pathway.html

Ishikawa, T., & Nakagawa, H. (2009). Human ABC transporter ABCG2 in cancer chemotherapy and pharmacogenomics. Journal of experimental therapeutics & oncology, 8(1), 5–24

Stonehouse, W., Gammon, C. S., Beck, K. L., Conlon, C. A., von Hurst, P. R., & Kruger, R. (2013). Kiwifruit: our daily prescription for health. Canadian Journal of Physiology and Pharmacology, 91(6), 442–447. https://doi.org/10.1139/cjpp-2012-0303

Collins, B. H., Horská, A., Hotten, P. M., Riddoch, C., & Collins, A. R. (2001). Kiwifruit protects against oxidative DNA damage in human cells and in vitro. Nutrition and cancer, 39(1), 148–153. https://doi.org/10.1207/S15327914nc391_20